Supplementary Figure 1. Cellular models employed in the colony formation assays.

a, The cancer type and the oncogenic alteration are given for each cellular model, as well as the targeted kinase inhibitor employed in each cell line and the corresponding IC_{50}. THZ1 IC_{50} is also shown. IC_{50} is based on dose-response curves determined by Cell-Titer Glo (at 96 hours). (NSCLC = non-small cell lung cancer)

b, Cell viability by Cell-Titer Glo (at 96 hours) with THZ1 over a range of doses. Mean (3 biological replicates) +/- SD shown, as a percentage of control.

a

Oncogene and cell line	Cancer type	Alteration	Targeted kinase inhibitor	TKI IC_{50} (nM)	THZ1 IC_{50} (nM)
FGFR					
H2077	NSCLC	FGFR1 amplification	BGJ398	10	10
RT112	Bladder	FGFR3-TACC3 fusion, FGFR3 amplification	BGJ398	8	107
EGFR					
H1975	NSCLC	EGFR L858R & T790M	WZ4002	155	275
HCC827	NSCLC	EGFR Exon 19 del E746-A750	erlotinib	6	76
PC9	NSCLC	EGFR Exon 19 del E746-A750	erlotinib	53	133
HER2					
N87	Gastric	HER2 amplification	lapatinib	42	41
OE19	Esophageal	HER2 amplification	lapatinib	128	80
MET					
EBC-1	NSCLC	MET amplification	crizotinib	7	26
PDGFR					
H1703	NSCLC	PDGFRA amplification	imatinib	244	11
ALK					
H3122	NSCLC	EML4-ALK fusion	crizotinib	247	33
KRAS					
A549	NSCLC	KRAS G12S	trametinib	40	240
GSU	Gastric	KRAS G12D	trametinib	1	100
H1792	NSCLC	KRAS G12C	trametinib	22	340
H2009	NSCLC	KRAS G12A	trametinib	9	21
H23	NSCLC	KRAS G12C	trametinib	11	60
BRAF					
A375	Melanoma	BRAF V600E	vemurafenib	305	64

b

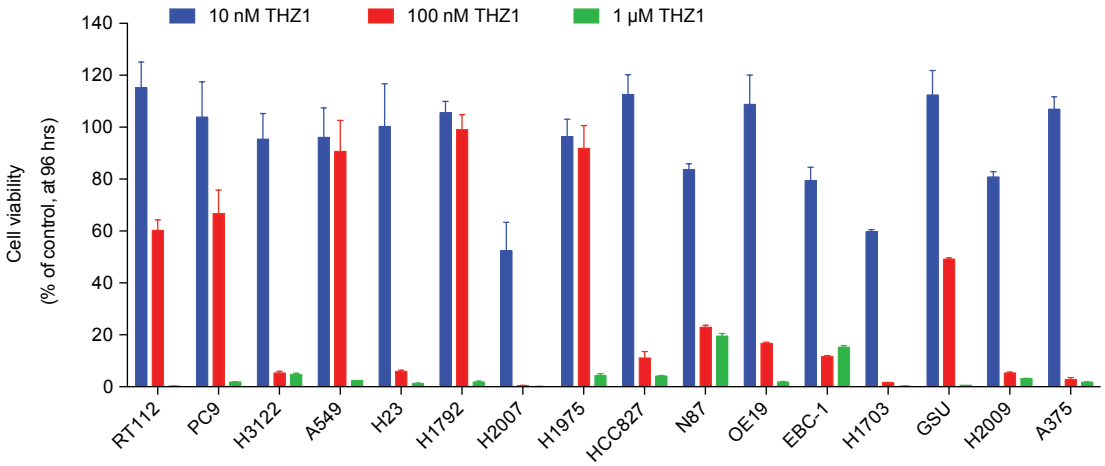

Supplementary Figure 1

Supplementary Figure 2. THZ1 in combination with targeted therapy enhances cell death and prevents establishment of drug resistant colonies in diverse oncogene-addicted cellular models.

a, Cellular models with diverse oncogene dependencies were treated with DMSO, the corresponding kinase inhibitor (TKI/MEKi/BRAFi) (see Supplementary Fig.1), THZ1, or THZ1 in combination with the targeted kinase inhibitor (Combo). Drug doses are provided in the Methods section. Colony formation was assayed by crystal violet staining at four weeks. Control wells were stained by one week. Three biological replicates were quantified and are shown here as a percentage of the control. Mean (3 biological replicates) +/- standard deviation (SD) shown (* p-value < 0.05, ** < 0.005, *** < 0.0005, two-sided t-test). ND = not detectable.

b, Cell death analysis for a subset of models in (a) by flow cytometry with Annexin V/PI staining, following 48 hours of treatment (H2077 shown at 24 hours, due to differences in response to drug time-course). Mean (3 biological replicates) +/- SD shown (* p-value < 0.05, ** < 0.005, *** < 0.0005, two-tailed t-test, considering total cell death (Annexin V+/PI- or PI+)). Left panel: OE19, middle panel: H2077, right panel: H1975.

c, Long-term colony formation for a subset of models presented in Figure 1. Colony formation was assayed at three months and quantified as in (a).

d, Colony formation with a mismatched kinase inhibitor (a kinase inhibitor not targeting the dependency of the cell line; vemurafenib used for RT112 and PC9, and crizotinib used for A549). Colony formation assay and quantification as in (a).

e, Cell viability, Cell-Titer Glo (96 hours), showing drug tolerant populations that remain with dual kinase inhibition targeting known resistance mechanisms in RT112, PC9 and H3122 (BGJ = BGJ398 (FGFR inhibitor), AZD = AZD8931 (pan-ERBB inhibitor), Tram = trametinib (MEK1/2 inhibitor), BKM = BKM120 (pan-PI3K inhibitor), Erlo = erlotinib (EGFR inhibitor), Criz = crizotinib (ALK and MET inhibitor), Lapa = lapatinib (EGFR and ERBB2 inhibitor), Lin = linsitinib (IGF-1R inhibitor) all at 1 μM, except crizotinib at 250 nM). THZ1 with targeted kinase inhibition shown for comparison (THZ1 at 150 nM, 100 nM, and 50 nM for RT112, PC9, and H3122, respectively). Mean (6 biological replicates) +/- SD shown.

f, Quantification of colony formation at four weeks for cells treated as in (e). Mean (3 biological replicates) +/- SD shown.

g, Quantification of colony formation at three months for the combinations that best restricted growth in (f) across the three cellular models. Mean (3 biological replicates) +/- SD shown.

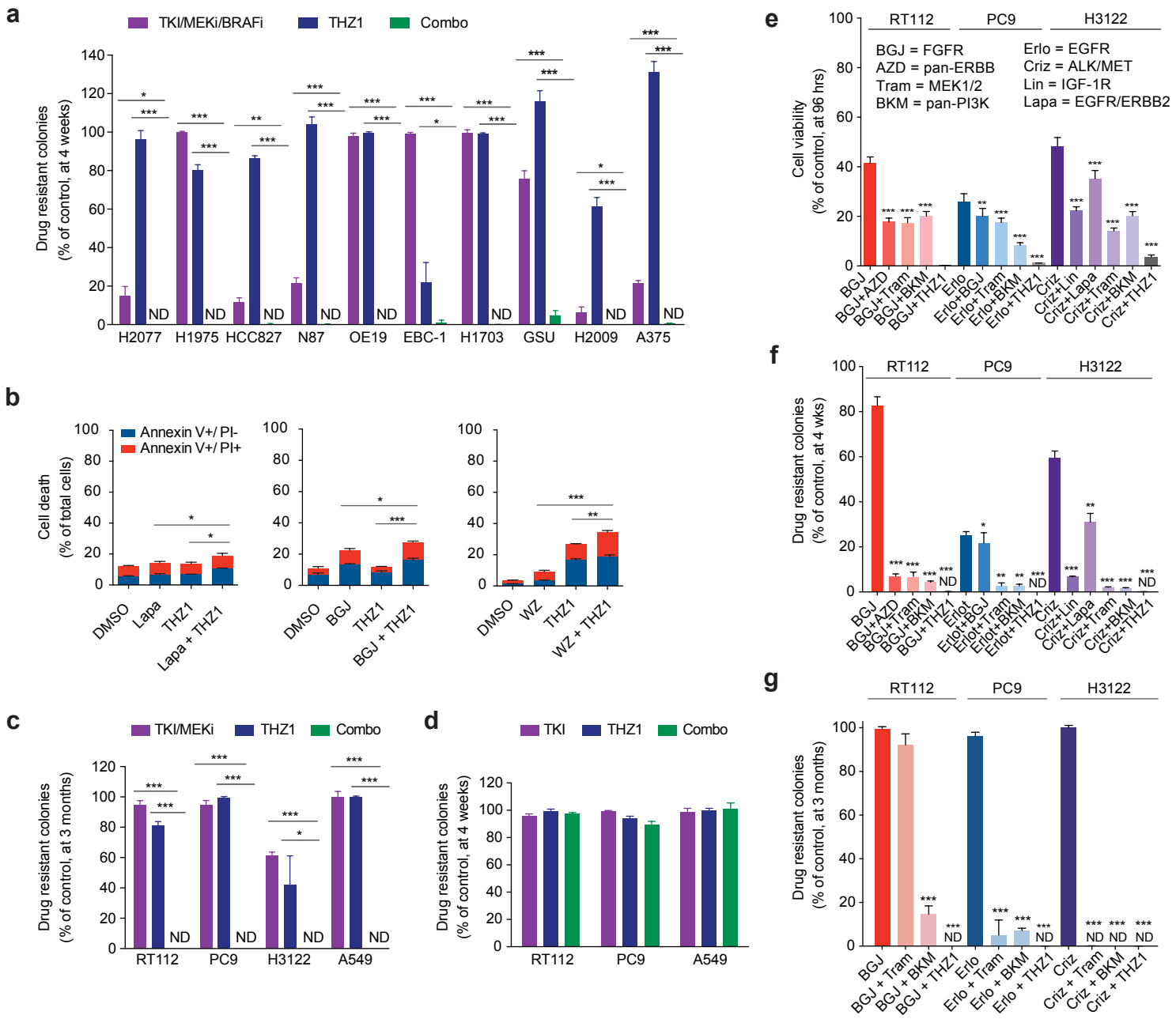

Supplementary Figure 2

Supplementary Figure 3. CDK7 or CDK12 knock-down in PC9 cells augments cell death in combination with erlotinib.

a, Relative CDK7 expression (qRT-PCR) following knockdown with three different CDK7 single guide RNAs (sgRNA) or a dummy guide in PC9 cells. Mean (3 biological replicates) +/- SD shown. Corresponding immunoblot showing decreased expression with CDK7 knockdown for the three different sgRNAs compared to the dummy guide. Similar results presented for CDK12.

b, Relative proliferation of PC9 cells following knockdown of CDK7 or CDK12 for the sgRNAs in (a) compared to the dummy guide. Mean (3 biological replicates) +/- SD shown.

c, Cell death analysis by flow cytometry with Annexin V/PI staining in CDK7 or CDK12 -deficient PC9 cells, following 48 hours of treatment with vehicle or erlotinib (1 μM). Mean (3 biological replicates) +/- SD shown (* p-value<0.05, **<0.005, *** <0.0005, two-tailed t-test, considering total cell death (Annexin V+/PI- or PI+), red asterix = compared to CDK7 or CDK12 sgRNA untreated, black asterix = compared to CDK7_12 dummy_Erlotinib).

d, Cell viability, Cell-Titer Glo (96 hours) for THZ531, a CDK12-selective inhibitor, showing dose response curves in RT112 and PC9. Mean (3 biological replicates) +/- SD shown.

e, Quantification of colony formation at four weeks, shown as a percentage of control, for RT112 and PC9 cells treated with DMSO, the corresponding tyrosine kinase inhibitor (TKI: BGJ398 at 1 μM , or erlotinib at 1 μM, for RT112 and PC9 respectively), THZ531 (100 nM for both RT112 and PC9), or THZ531 in combination with the corresponding TKI. Control wells were stained by

one week. Three biological replicates were quantified and are shown here as a percentage of the control. Mean (3 biological replicates) +/- standard deviation (SD) shown (* p-value < 0.05, ** < 0.005, *** < 0.0005, two-sided t-test). ND = not detectable.

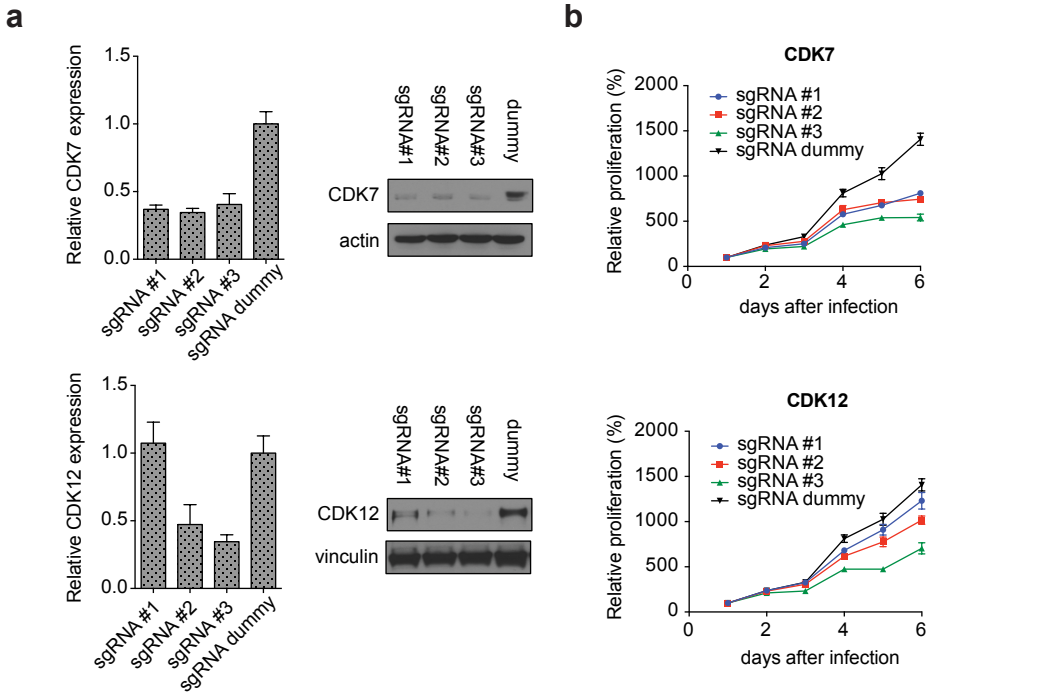

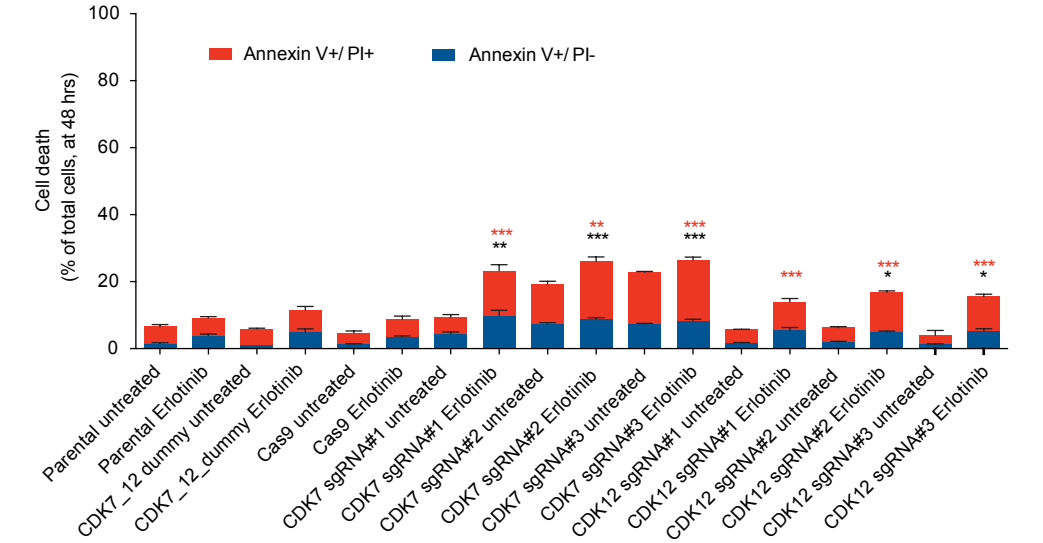

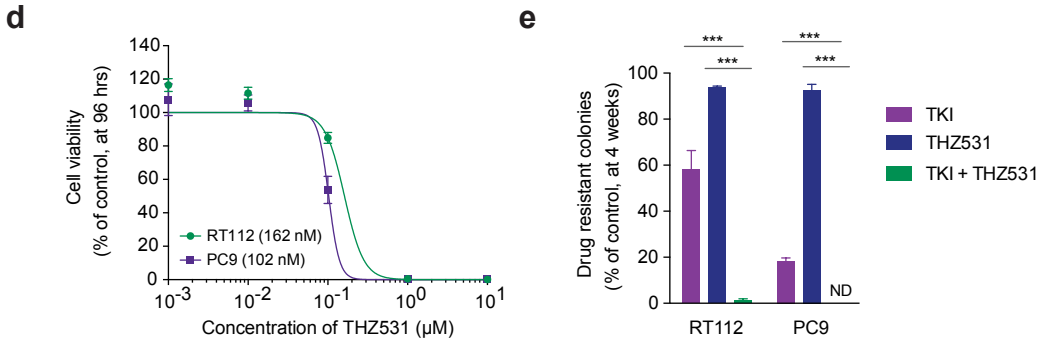

Supplementary Figure 3

Supplementary Figure 4. THZ1 in combination with targeted therapy induces significant tumor regression in diverse xenograft models and an EML4-ALK-driven GEMM.

a, Tumor volume index for mice with RT112 and PC9 xenografts treated with the indicated drugs for 8 weeks (n=5 mice in each treatment group, equivalent to 10 tumors in each group). Number of tumors indicated above each bar. (* mouse censored, see methods for details)

b, Tumor volume index normalized to pre-treatment volume for mice with EML4-ALK- driven-NSCLC treated with vehicle, crizotinib, THZ1, or THZ1 in combination with crizotinib. Mice in the combination-treated arm had significant tumor regression compared to mice treated with crizotinib alone (* p-value < 0.05, two-sided t-test).

c, Representative MRI images for mice treated with vehicle, crizotinib, THZ1 or the combination of the two, pre-treatment, at week 2 and at week 4, showing significant tumor regression with combination treatment. Heart and tumor areas are drawn up and marked with yellow and red lines, respectively.

d, Weights (grams) of xenograft and GEMM mice over study duration.

e, Target engagement in mouse tumor and liver tissues. Mice were treated for 72 hours with vehicle or THZ1 10 mg/kg BID i.p., and tissue was harvested 6 hours following the last dose. Lysates prepared from homogenized tissue were incubated with bio-THZ1. Streptavidin-conjugated beads

were used to pull down bio-THZ1 complexed with CDK7. CDK7 target engagement in pulldown lysates was analyzed by immunoblotting with antibodies for CDK7.

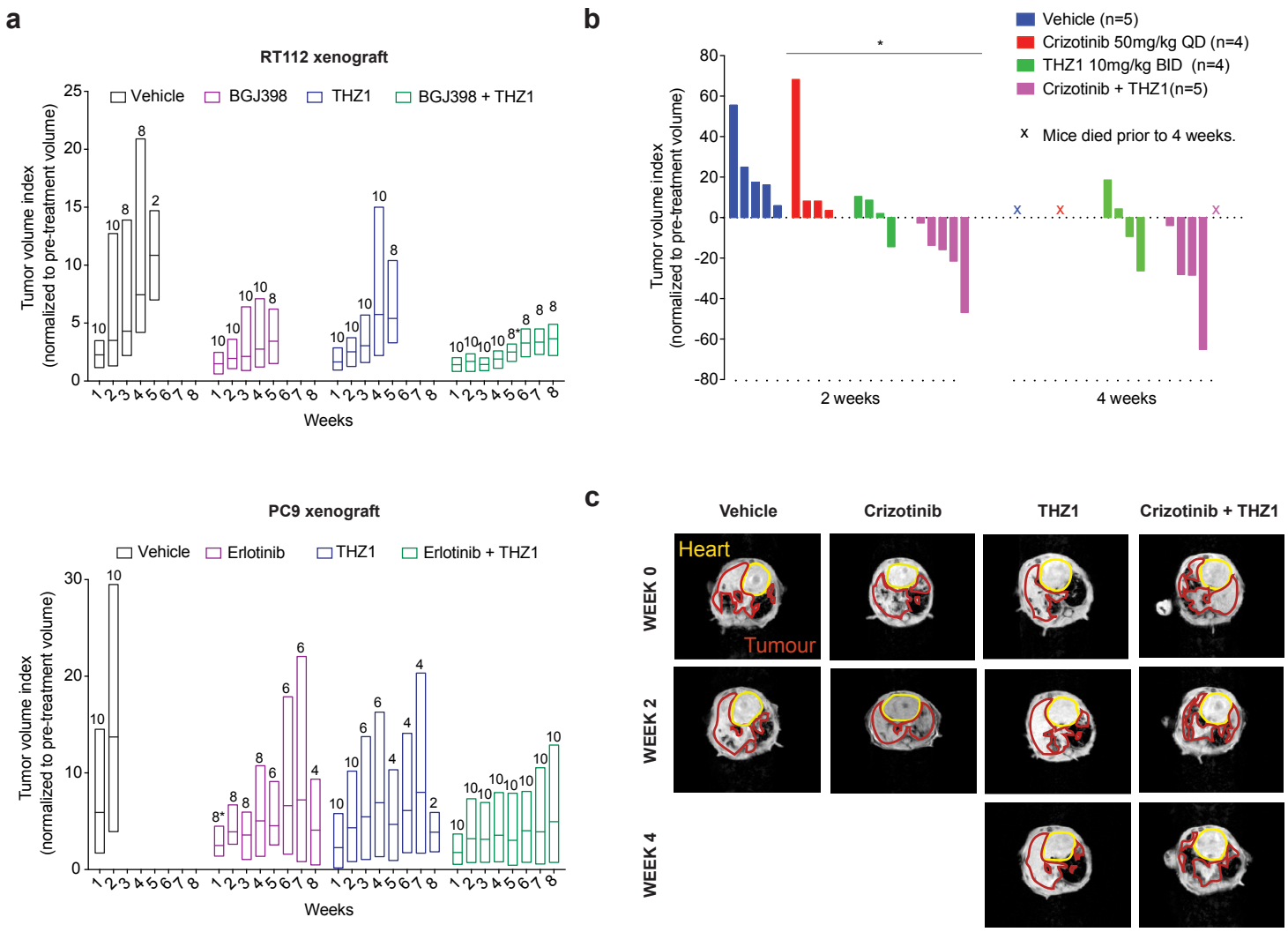

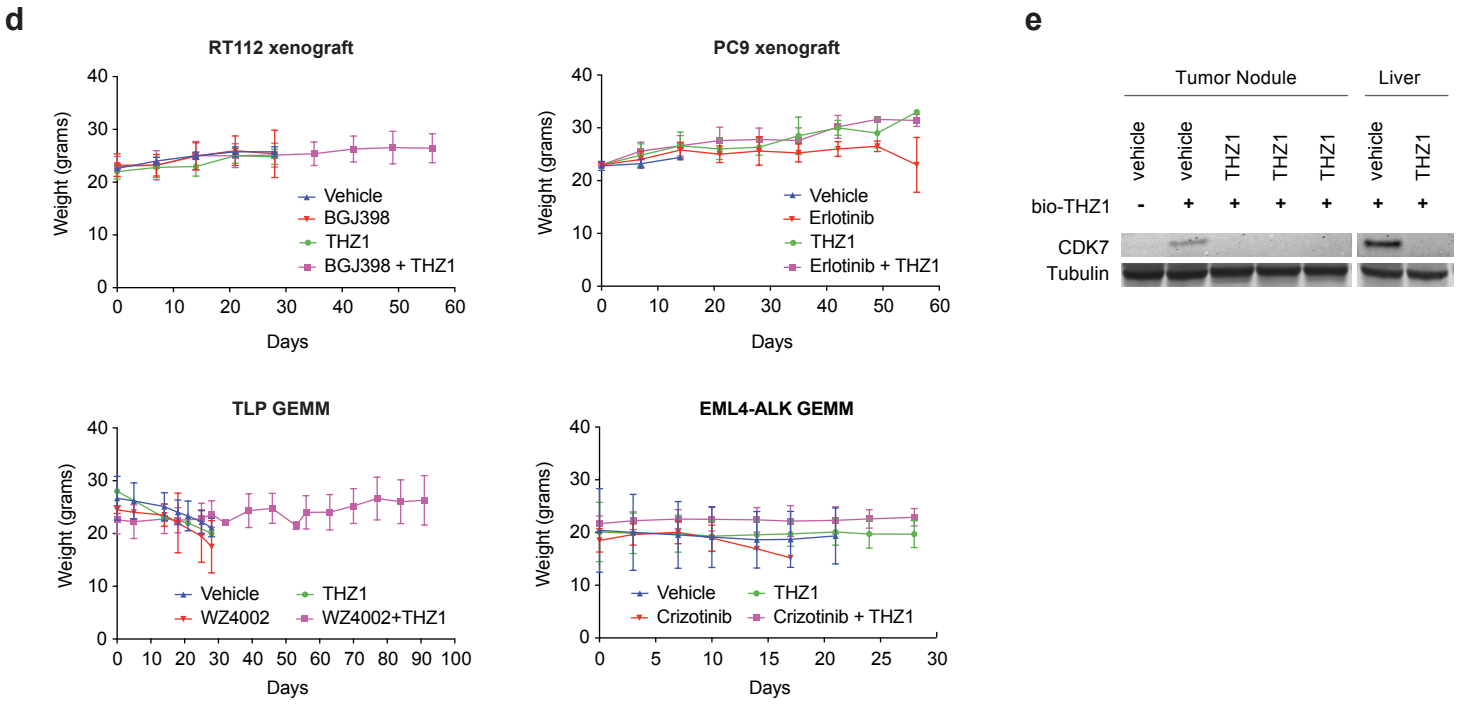

Supplementary Figure 4

Supplementary Figure 5. THZ1 attenuates the transcriptional responses engaged by targeted therapy in diverse cellular models.

a, Differentially expressed genes at 48 hours following treatment with THZ1, TKI or MEKi, or THZ1 in combination with TKI or MEKi (Combination, C) compared to DMSO control (D), filtered by genes that were up- or downregulated greater than or equal to 1.5 log2-fold change (LFC) of read counts per million with targeted kinase inhibition, or less than or equal to -1.5 LFC, respectively. Column four shows LFC of combination-treated versus targeted therapy-treated cells (C/TKI, C/MEKi). Heat maps show averaged values for 3 biological replicates per condition. The number of upregulated and downregulated genes (LFC ≥1.5, and ≤ -1.5, respectively) for each condition is summarized below each column, in red and blue respectively. LFC values between -1.5 and 1.5 are shown in white.

b, Supervised analysis of highly differentially expressed genes following treatment with targeted therapy. Heat maps show LFC of read counts per million (3 biological replicates per condition) for THZ1/DMSO (THZ1/D) at 48 hours, targeted therapy/DMSO (TKI/D, BRAFi/D, or MEKi/D) at 48 hours and 7 days, and combination treatment/DMSO (C/D) at 48 h. Genes are organized by pathways previously identified in the literature as having a role in facilitating resistance emergence.

c, Differentially expressed genes following treatment with targeted therapy for 48 hours and 7 days compared to control (LFC of read counts per million, 3 biological replicates per condition, filtered

by genes that were up- or downregulated greater than or equal to 1.5 LFC with targeted kinase inhibition at 48 hours, or less than or equal to -1.5 LFC, respectively).

d, Violin plots showing changes in gene expression for combination- versus targeted therapy-treated cells (LFC C/TKI) for genes that were upregulated (Up, red), downregulated (Down, blue), or unchanged by targeted kinase inhibition (NC, yellow). A LFC ≥1.5, and ≤ -1.5, was used to define up- and downregulated genes, respectively. The number of genes in each plot is indicated. Combination treatment resulted in significantly different expressions for genes up- and down-regulated by targeted therapy in all six cellular models tested (Mann-Whitney U, p-value shown above each plot).

e, Overall gene expression changes (LFC) for targeted therapy-treated cells (TKI) and THZ1-treated cells compared to DMSO. Red indicates upregulated genes (LFC ≥1.5). Blue indicates downregulated genes (LFC ≤ -1.5). Grey indicates LFC values between -1.5 and 1.5.

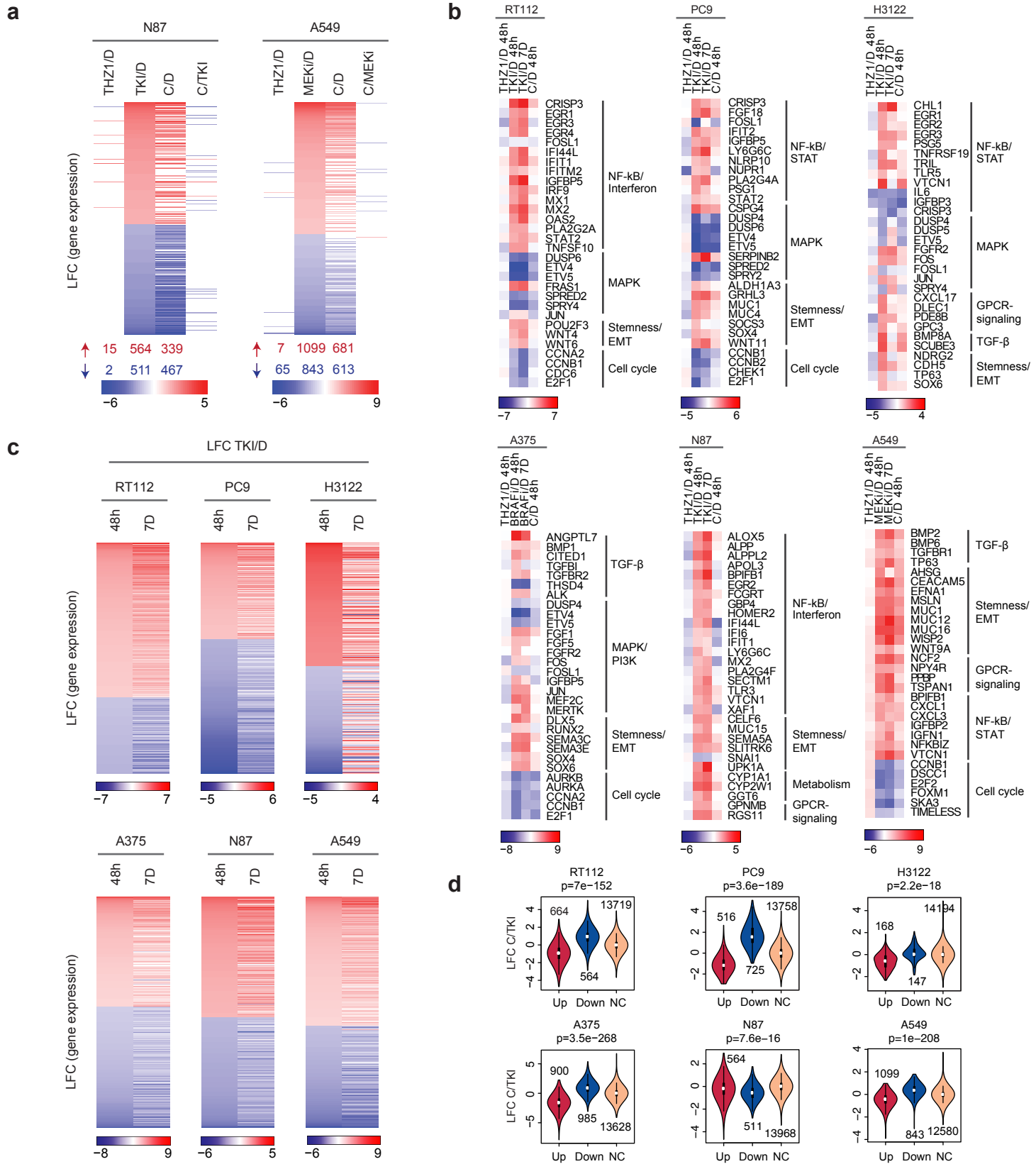

Supplementary Figure 5

Supplementary Figure 6. EGR1 knockdown phenocopies effect of THZ1 in combination with targeted therapy.

a, Immunoblot showing decreased expression with EGR1 knockdown for three different sgRNAs compared to the dummy guide.

b, Quantification of colony formation with EGR1-deficient cells, shown as a percentage of the control. Mean (3 biological replicates) +/- standard deviation (SD) shown. P-value represents pairwise comparisons for each sgRNA compared to control (sg Dummy) for each particular treatment arm (* p-value < 0.05, ** < 0.005, *** < 0.0005, two-sided t-test).

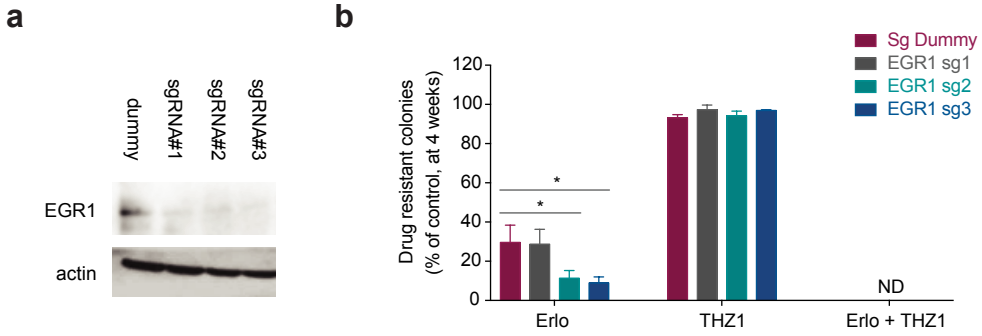

Supplementary Figure 6

Supplementary Figure 7. Top upregulated genes in combination-treated cells vs. targeted therapy-treated cells.

a, Heat map of the most highly upregulated genes in combination-treated cells vs. targeted therapy-treated cells across the six cellular models employed, considering only genes whose expression was upregulated more than or equal to 1.5 LFC CPM (C/TKI). Genes in bold are histone proteins. Columns on the right indicate the number of cell lines with LFC>1.25, and LFC>1.5 for each respective gene.

a

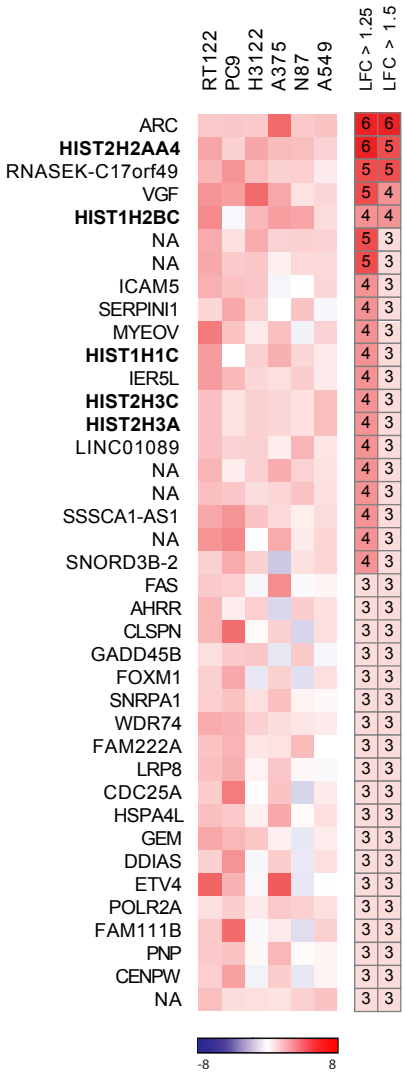

Supplementary Figure 7

Supplementary Figure 8. THZ1 attenuates the redistribution of BRD4 signal elicited by targeted kinase inhibition in diverse cellular models.

a, LFC of BRD4 ChIP-seq signal at super-enhancer regions (SE) following 48 hour treament with THZ1, targeted-therapy (TKI, MEKi) or THZ1 in combination with targeted therapy (C) compared to DMSO control (D). The fourth column shows combination treatment compared to targeted therapy treatment (C/TKI, C/MEKi). The heat map plots the union of SE regions identified in DMSO-treated cells and targeted therapy-treated cells. The number of upregulated and downregulated regions is summarized below each column, in red and blue respectively. Violin plots show the distribution of LFC of BRD4 ChIP-seq density at super-enhancer regions plotted in the heat maps, for TKI compared to DMSO, combination treatment compared to targeted therapy treatment and combination compared to DMSO.

b, Violin plots showing the distribution of LFC of BRD4 ChIP-seq density at typical enhancers (TE) following 48 hours of treatment as indicated.

c, BRD4 density at SE regions following 48 hours of treatment as indicated.

d, Heat maps of LFC BRD4 ChIP-seq density at SE regions following treatment for 48 hours with the corresponding targeted therapy compared to control, and LFC H3K27ac ChIP-seq density at these regions following treatment for 7 days (7D).

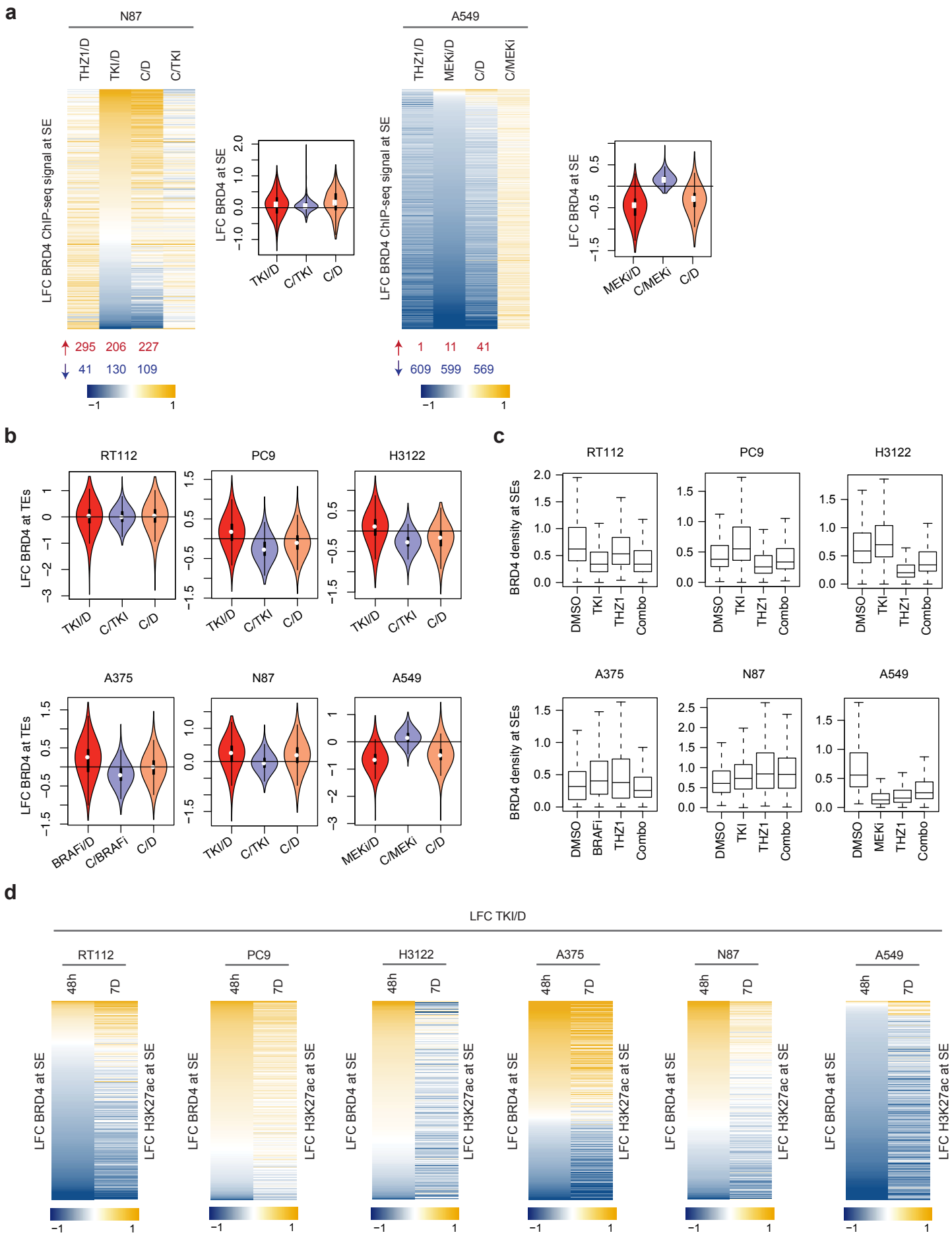

Supplementary Figure 8

Supplementary Figure 9. Enhancer status parallels gene expression levels.

a, Gene expression (log2 of read counts per million (CPM)) for genes with super-enhancers (SE), typical enhancers (TE), and no active enhancer (remaining genes, RG). Super-enhancer-regulated genes had significantly higher gene expression compared to those with typical enhancers and those with no active enhancer. Genes with typical enhancers had significantly higher gene expression compared to those without enhancer signal (* p-value<0.05, **<0.005, *** <0.0005, two-tailed t-test).

b, Super-enhancers were separated into three equally sized groups (A,B,C) based on their BRD4 fold-changes and were each assigned to the proximal active gene. Group A represents those with the lowest BRD4 fold-changes, and C those with the highest fold changes. The distributions of gene expression (LFC of read counts per million) for each group are plotted as boxplots. First and third quartiles, and median are shown. The whiskers represent 1.5 times the interquartile range (p-value given, one-way ANOVA comparing groups A, B and C for each condition).

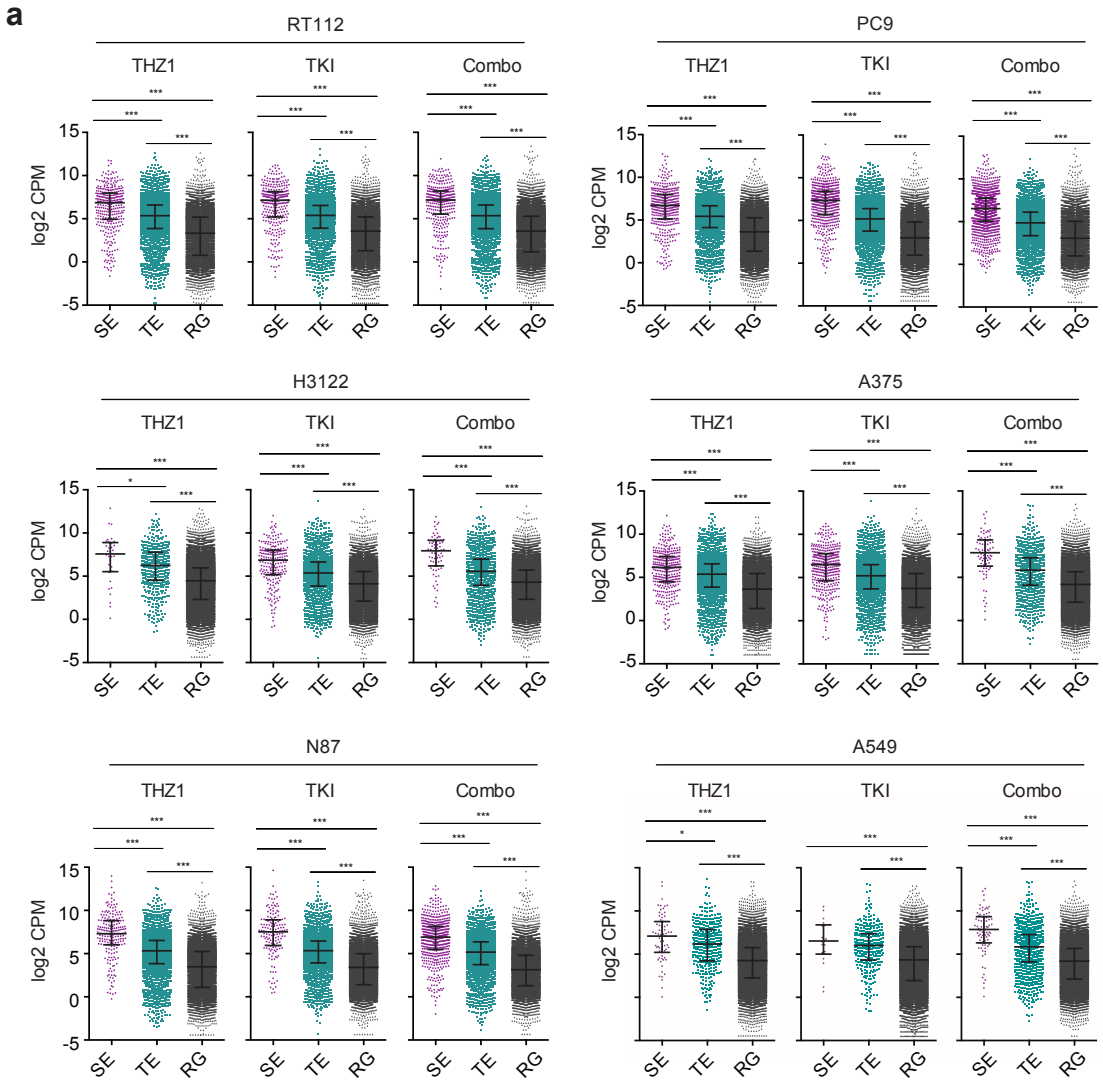

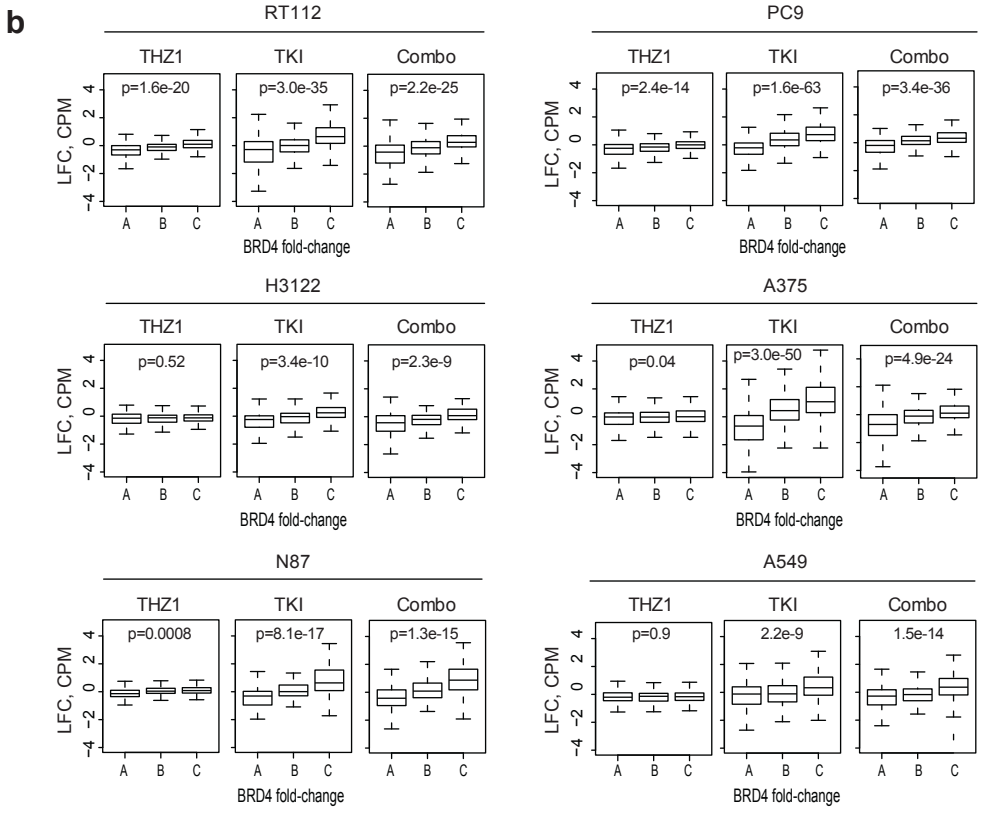

Supplementary Figure 9

Supplementary Figure 10. Combination treatment with THZ1 plus a kinase inhibitor results in more complete suppression of ERK activity than kinase inhibition alone, and forced reactivation of the MAPK pathway results in observable rescue from both kinase inhibition alone and combined THZ1-kinase inhibition.

a, Immunoblot analysis for AKT and ERK activity for cells treated with control, THZ1, the corresponding kinase inhibitor (TKI or MEKi), or combination treatment for 24 hours, at doses used for colony formation assays.

b, Immunoblot showing absent expression of NF1 with knockdown of NF1 by three different sgRNAs compared to a dummy guide.

c, Immunoblot showing decreased expression of SPRED2 with knockdown of SPRED2 by three different sgRNAs compared to a dummy guide.

d, Colony formation for PC9 cells with a sgRNA dummy guide, or knockdown of NF1 or SPRED2 by three different guides. Cells were treated with DMSO, erlotinib (Erlo), THZ1, or THZ1 in combination with erlotinib. Colony formation was assayed by crystal violet staining at two weeks. DMSO was stained by 1 week. Two representative wells from a minimum of three biological replicates are shown per condition (erlotinib 100 nM, THZ1 50 nM).

e, Quantification of colony formation in (d), shown as a percentage of the control. Mean (3 biological replicates) +/- standard deviation (SD) shown. P-value represents pairwise comparisons

for each sgRNA compared to control (sg Dummy) (* p-value < 0.05, ** < 0.005, *** < 0.0005, two-sided t-test).

f, Immunoblot of ERK activity for PC9 cells transduced with sgRNA dummy guide, or the NF1 or SPRED2 guide conferring the greatest rescue from erlotinib in (d). Cells were treated with control, THZ1, erlotinib, or combination treatment for 24 hours, at doses used for colony formation assays in (d).

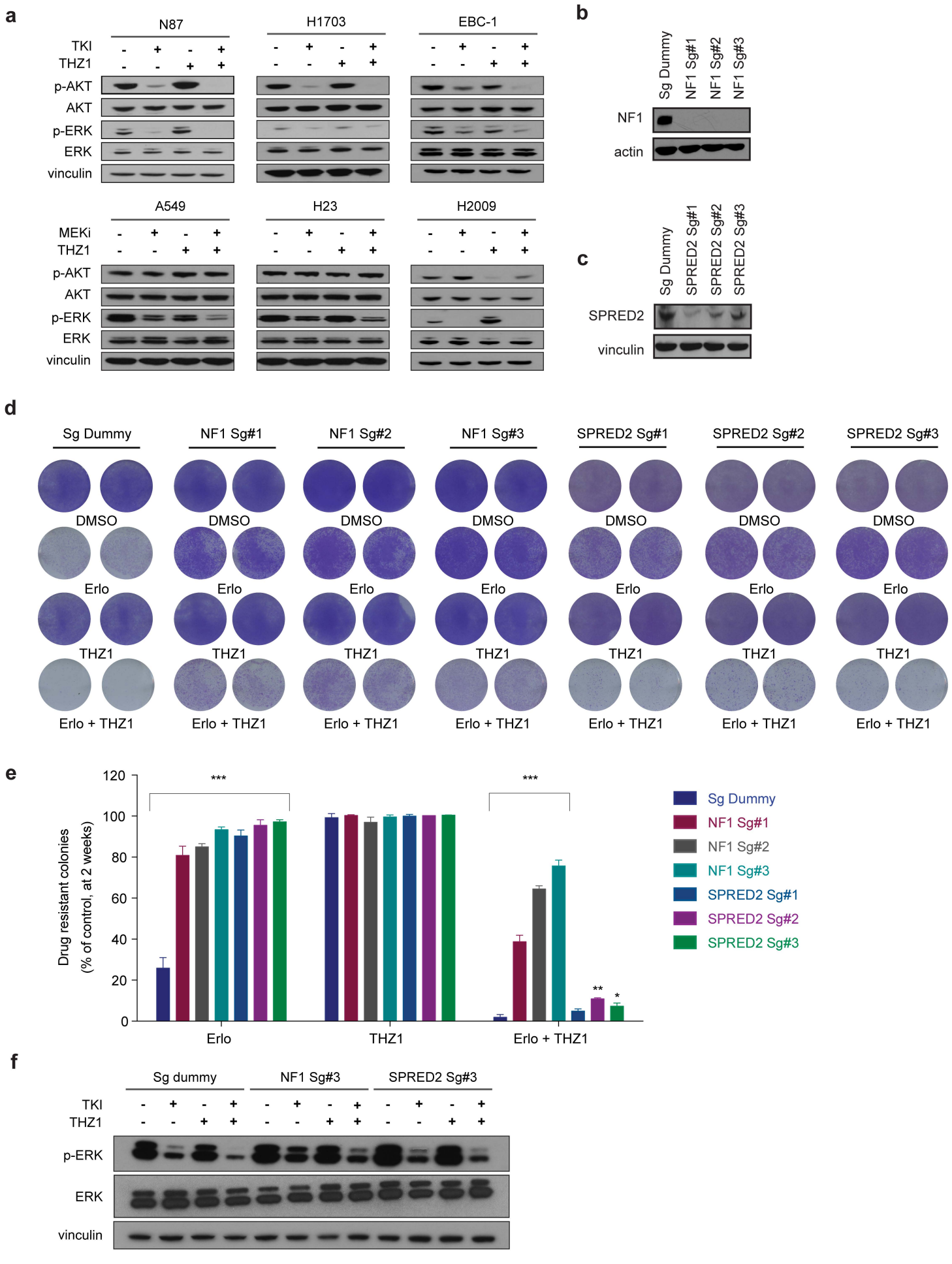

Supplementary Figure 10